scientific reports

Check for updates

OPEN

Immunomodulatory therapy with glatiramer acetate reduces endoplasmic reticulum stress and mitochondrial dysfunction in experimental autoimmune encephalomyelitis

Tapas K. Makar[1,2]✉, Poornachander R. Guda[1], Sugata Ray[1], Sanketh Andhavarapu[1], Kaspar Keledjian[3], Volodymyr Gerzanich[3], J. Marc Simard[3], Vamshi K. C. Nimmagadda[1] & Christopher T. Bever Jr[1,2,4]

Endoplasmic reticulum (ER) stress and mitochondrial dysfunction are found in lesions of multiple sclerosis (MS) and animal models of MS such as experimental autoimmune encephalomyelitis (EAE), and may contribute to the neuronal loss that underlies permanent impairment. We investigated whether glatiramer acetate (GA) can reduce these changes in the spinal cords of chronic EAE mice by using routine histology, immunostaining, and electron microscopy. EAE spinal cord tissue exhibited increased inflammation, demyelination, mitochondrial dysfunction, ER stress, downregulation of NAD+ dependent pathways, and increased neuronal death. GA reversed these pathological changes, suggesting that immunomodulating therapy can indirectly induce neuroprotective effects in the CNS by mediating ER stress.

Multiple sclerosis (MS) is a disease of the central nervous system (CNS), characterized pathologically by inflammation, demyelination, axonal damage and neuronal loss[1]. These events are triggered by heterogenous myelin-reactive peripheral immune cells infiltrating the blood–brain-barrier (BBB)[2]. The most widely used animal model for MS is experimental autoimmune encephalomyelitis (EAE), a murine model characterized by CNS inflammation, demyelination, axonal transection, and neurological impairment due to infiltration of auto-reactive cells[3–7]. Currently available disease-modifying therapies for MS have not been proven to prevent or reverse long-term neurodegeneration[8,9], although they have been shown to reduce inflammation[10]. Yet, pathological axonal damage[6] and neuronal loss[11] in the brain and spinal cord atrophy on magnetic resonance imaging (MRI) scans are highly correlated with long-term disability and progression more so than inflammation[12]. Therefore, a large focus of current MS research is currently seeking to better understand the mechanisms underlying neurodegeneration in MS to guide the development of neuroprotective therapies that promote myelin repair.

Pathological studies of MS lesions have implicated mitochondrial dysfunction in MS associated neurodegeneration[13]. MRI spectroscopy shows changes in N-acetyl aspartate levels consistent with decreased mitochondrial function in acute lesions[14,15]. The proximate cause of this mitochondrial dysfunction is unknown, but could be linked to endoplasmic reticulum (ER) stress[16,17]. Mitochondria and the ER are anatomically linked through a region of the ER known as the mitochondria associated membrane (MAM) and functionally by the release of calcium and other mediators[18–21]. This has shifted research focus towards the effects of inflammation on endoplasmic reticulum stress and mitochondrial function. ER stress has been previously shown to promote the Th17 response and upregulate proinflammatory cytokines such as IL-6[22].

[1]Department of Neurology, School of Medicine, University of Maryland, College Park, USA. [2]Research Service, Institute of Human Virology, VA Maryland Health Care System, 725 W Lombard St, Baltimore, MD 21201, USA. [3]Department of Neurosurgery, School of Medicine, University of Maryland, College Park, USA. [4]Department of Veterans Affairs, Office of Research and Development, Washington, USA. ✉email: sandhava@umd.edu

Glatiramer Acetate (GA), commonly known as copaxone, is an approved immunomodulatory disease-modifying drug for MS treatment[23]. GA mediates demyelination by altering T-cell differentiation and inducing a shift towards Th2/3 cells and neurotrophic factors that can penetrate the blood–brain-barrier (BBB) and accumulate in the CNS[24–27]. To date, the effects of GA on ER stress and mitochondrial dysfunction in the CNS of EAE mice have not been studied, so we set out to investigate this. Using routine histology, immunohistochemistry, western blotting, and electron microscopy, we discovered that GA mediates ER stress, mitochondrial function and dynamics, and NAD+ dependent pathways. Our findings elucidate that targeting ER stress through a peripherally acting drug can be neuroprotective in MS.

Methods

Animals. Female C57Bl/6J mice were obtained from The Jackson Laboratory (Bar Harbor, ME, USA). Mice were housed in our facilities under pathogen-free conditions at the University of Maryland, School of Medicine, Baltimore. All experimental protocols were approved by the University of Maryland Institutional Animal Care and Use Committee. All methods were carried out in accordance with NIH guidelines and the recommendations in the ARRIVE guidelines.

EAE induction. EAE was induced in eight week old female C57Bl/6 mice with 0.2 mg of the MOG 35–55 peptide in complete Freund's adjuvant (CFA) followed by pertussis toxin injections as we have described previously[28,29].

Clinical evaluation. Mice were scored daily by blinded raters using a standard impairment scale as described previously[28].

Drug treatment. Glatiramer Acetate (GA) (TEVA Neuroscience) was administered subcutaneously at a dose of 125 µg/mouse/day in a 200 µl vehicle of phosphate-buffered saline (PBS). The mice were randomized to vehicle-treated EAE (EAE), GA-treated EAE (EAE + GA) and vehicle-treated age matched normal female mice. All mice received a single injection daily starting from the day of disease onset among the EAE mice (Score ≥ 1).

Tissue pathology. Mice were euthanized on day 60 using general anesthetic isoflurane, and spinal cords and brains were removed and prepared for histology and analyzed as described previously[28,30]. 7 µm thick sections were stained with hematoxylin and eosin (H&E) (to detect inflammatory infiltrates) and Luxol Fast Blue (for demyelination) following standard protocols for conventional light microscopy.

Immunohistochemistry. Immunohistochemical studies were carried out as described previously[28,31]. Immunohistochemistry was performed using VECTASTAIN ABC kits (Vector Laboratories, Burlingame, CA, USA). 7 µm thick sections were used. Nuclei were counterstained with hematoxylin. Slides were examined using standard brightfield microscopy. The primary antibodies used are listed in Table 1.

Immunofluorescence. Immunofluorescence studies were carried out as described previously[28,32]. 7 µm thick paraffin sections were deparaffinized in xylene, rehydrated through graded alcohols to water, washed in 0.01 M PBS, preincubated with 10% donkey serum for 60 min, and then incubated overnight at 4 °C with primary antibody diluted in PBS with 1% bovine serum albumin (BSA) together with 0.3% Tween-20. The primary antibodies used are listed in Table 1. The specificity of the immunostaining for all the proteins was tested in control slides by incubation with pre-immune pre-adsorption of the antibody with the respective peptides used as immunogens. Slides were examined using standard fluorescence microscopy and results were quantitated by counting fluorescent cells per area or field.

TUNEL assay for apoptotic cell death. ApopTag Peroxidase Kit (Chemicon International, Temecula, CA) was used to assess the extent of cell death in the spinal cord sections of EAE animals and GA treated animals. Briefly, all the slides were deparaffinized with xylene and rehydrated through graded alcohols to water, washed in 0.01 M PBS then pretreated with a protein-digesting enzyme for 15 min and then washed with water for 2 min. slides were treated with 3% (v/v) hydrogen peroxide for 5 min followed by washing with PBS. Terminal deoxynucleotidyl transferase (TdT) enzyme was added to the pre-equilibrated spinal cord sections and incubated for 1 h at 37 °C. Stop-buffer was added to the slide and agitated for 15 s followed by 10 min incubation at room temperature. After washing three times with PBS for 1 min each, anti-digoxigenin peroxidase conjugate was added to the slides and incubated for 30 min. After slides were washed twice with PBS, freshly prepared peroxidase substrate 3,3′-diaminobenzidine was added to the slides and kept for 6 min and then slides were washed with water three times. Slides were counterstained with 0.5% (w/v) DAB for 5 min followed by washing with water and then 100% n-butanol. After 10 min, cells were dehydrated in xylene for 2 min and then mounted with glass coverslip. Experiments were conducted in triplicates and the ApopTag-positive cells was determined by counting cells under light microscopy.

Analysis of histological images using Image J. Image J was used for histological quantification by a blinded observer[33]. Cell infiltration was quantitated by counting the number of positive quadrants with inflammation, and then expressed as a percentage over the total number of quadrants examined in the histogram as reported previously[28]. Demyelination was quantitated using LFB staining and MBP staining as described previously[28]. The cell labeling experiments (IL-17, IFN-γ, Cytochrome C, PINK-1, PERKIN, DNM1-L, PGC-

Antibody	Target	Vendor	Concentration
Anti-IFN-y	Pro-inflammatory cytokine	Bioss, Woburn, MA, USA	1:100(IHC)*
Anti-IL-17	Pro-inflammatory cytokine	Santa Cruz Biotechnology, Santa Cruz, CA, USA	1:50(IHC)
Anti-MBP	Myelin basic protein	Abcam, Cambridge, MA, USA	1:500(IF) **
Anti-MFN-2	Mitofusin-2	Abcam, Cambridge, MA, USA	1:400(IF)
Anti-Fis-1	Mitochondrial fusion	BioVision, Milpitas, CA, USA	1:100(IF)
Anti-DNM1-L	Dynamin-like protein	Life Span Biosciences, Seattle, WA, USA	1:600(IHC)
Anti-PGC1-α	Peroxisome proliferator-activated receptor gamma coactivator 1-alpha	Abcam, Cambridge, MA, USA	1:500(IHC)
Anti-FOXO-1	Forkhead box protein O1	Santa Cruz Biotechnology, Santa Cruz, CA, USA	1:100(IHC)
Anti-TFAM	Mitochondrial transcription factor A	Bioss, Woburn, MA, USA	1:1000(IHC)
Anti-Cytochrome C Oxidase	Cytochrome C release	Abcam, Cambridge, MA, USA	1:50 (IHC)
Anti-SIRT-1	Sirtuin 1	Life Span Biosciences, Seattle, WA, USA	1:500(IHC)
Anti-SIRT-3	Sirtuin 3	Santa Cruz Biotechnology, Santa Cruz, CA, USA	1:100(IHC)
Anti-NAMPT	Nicotinamide phosphoribosyltransferase	Novus Biologicals, Littleton, CO, USA	1:100(IHC)
Anti-BAX	Pro apoptotic marker	Life Span Biosciences, Seattle, WA, USA	1:2000(IHC)
Anti-CHOP	Endoplasmic reticulum stress marker	Life Span Biosciences, Seattle, WA, USA	1:500(IHC)
Anti-PERK	Endoplasmic reticulum stress marker	Abcam, Cambridge, MA, USA	1:500(IHC)
Anti-PARKIN	Mitophagy marker	Novus Biologicals, Littleton, CO, USA	1:500(IHC)
Anti-PINK1	Mitophagy marker	Abcam, Cambridge, MA, USA	1:200(IHC)
Anti-VDAC-1	Mitochondrial Membrane protein marker	Abcam, Cambridge, MA, USA	1:500(IHC)
Anti-PACS2	Mitochondrial Membrane protein marker	Boster, Pleasanton, CA, USA	1:500(IHC)

Table 1. List of antibodies used in the study.

1alpha, TFAM, CHOP, PERK, PACS-2, VDAC-1, NAMPT, SIRT-1, SIRT-3, FOXO-1, BAX, MBP, NFM-2, Fis-1) were quantified based on the number of positive cells/field (200X or 400X). All fields covering the entire white matter (10–12 fields/section) and gray matter (5–7 fields/section) were analyzed from each spinal cord. The cell counting and data analysis were performed by an examiner blinded to treatment assignment.

Electron microscopy. Spinal cords were excised and fixed with a solution of 2% paraformaldehyde, 2.5% glutaraldehyde, in 0.1 M PIPES buffer (pH 7) at 4 °C overnight. Specimens were washed with 0.1 M PIPES buffer (pH 7), treated with 50 mM glycine in 0.1 M PIPES buffer for 15 min and washed again with 0.1 M PIPES buffer. Tissue pieces were then post-fixed in 1% osmium tetroxide, 1.5% potassium ferrocyanide in 0.1 M PIPES buffer for 60 min, washed and followed by en bloc staining with 1% (w/v) uranyl acetate for 60 min. After washing, specimens were dehydrated using a serial graded ethanol solution (30%, 50%, 70%, 90% and100%) and then 100% acetone. After dehydration, specimens were infiltrated and embedded in Araldite resin (Electron Microscopy Sciences, PA) following manufacturer's recommendation. Ultra-thin sections ~ 70 nm thickness were cut on a Leica UC6 ultramicrotome (Leica Microsystems, Inc., Bannockburn, IL) and collected onto copper grids and examined in an FEI Tecnai T12 transmission electron microscope (FEI. Co., Hillsboro, OR) operated at 80 kV. Digital images were acquired by using a bottom mount CCD camera (Advanced Microscopy Techniques, Corp, Woburn, MA) and AMT600 software (AMT, Woburn, MA, USA). A minimum of 3 different grids were examined for each animal from each group (N = 5). All the grids were examined at × 1100 for identification of white matter and gray matter and then examined at higher magnification for mitochondrial structure and endoplasmic reticulum integrity (× 6,500 and × 11,000).

Statistical analysis. Data analysis was performed using Prism software (Graph Pad, San Diego, CA) and groups were compared using one-way analysis of variance (ANOVA) with Fisher's protected least significant difference (PLSD) post hoc test at a 95% confidence interval. All results were presented as mean ± standard error of mean (SEM) of separate experiments (n ≥ 5). Differences were considered significant at $P \leq 0.05$.

Results

Glatiramer Acetate treatment improves clinical score, reduces demyelination, and suppresses inflammation in EAE mice (Fig. 1). *Clinical score* All mice developed clinical symptoms at about post immunization day (p.i.d.) 9 (± 2.0) and without treatment average clinical scores remained elevated through p.i.d. 30 (Fig. 1A1). GA treatment started at the time of symptom onset reduced the severity of disease within three days and scores remained significantly lower than the untreated EAE group with average clinical scores over days 10 to 30 of 0.57 ± 0.06 compared with 1.8 ± 0.15; $P < 0.0001$ (Fig. 1A2).

Production of pro-inflammatory cytokines was examined by immunohistochemical staining for interleukin-17 (IL-17) (Fig. 1C1–C3) and interferon-gamma (IFN-g) (Fig. 1C5–C7). The number of cells expressing IL-17 was

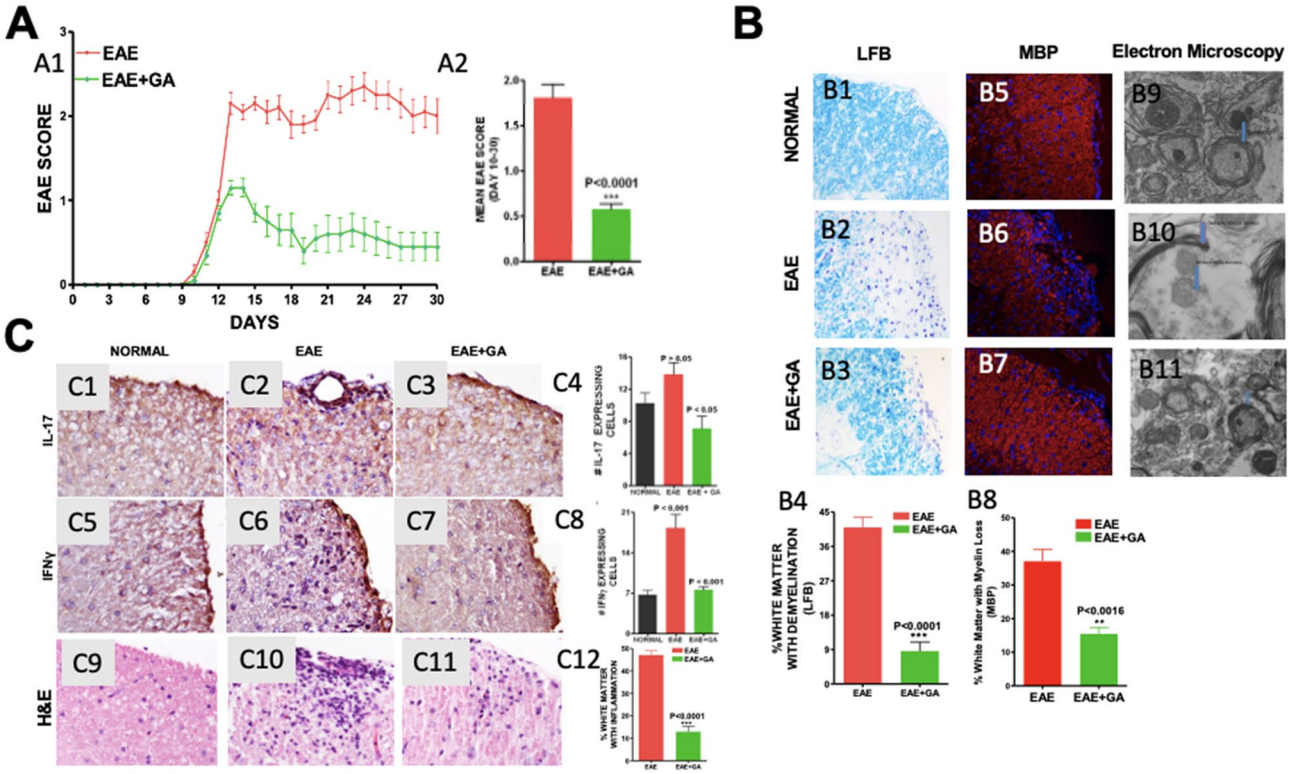

Figure 1. Glatiramer Acetate treatment improves clinical score, reduces demyelination, and suppresses inflammation in EAE mice. (1**A**) Graph of mean EAE scores for both groups of mice over a 30-day period. (1A1) The clinical severity of EAE disease was reduced by GA treatment. (1A2) Mean score for all animals in each group during the disease phase (days 10–30). The mean score was significantly lower in the GA treated EAE (EAE + GA) mice ($P < 0.0001$) compared to untreated EAE mice. N = 20/group, t-test. (**B**) Demyelination in EAE was reduced by GA treatment. Demyelination was assessed on LFB-stained (1B1–1B3) and MBP stained (1B5–1B7) sections of spinal cord white matter. Original magnification was × 400. B4 and B8 are graphs of the number of quadrants with demyelination expressed as a percentage of the total number of quadrants examined (n = 4), with statistics based on the t-test. B9–B11 shows transmission electron microscographs (TEM) at 6500 × magnification in normal mouse (1B9) untreated EAE mice (1B10) and EAE with GA treatment (1B11). These images are representative of at least 3 grids from each of five mice in each group. (1**C**) Inflammation in EAE was reduced by GA treatment. Inflammation was assessed in spinal cord white matter by (1C1–1C4) cells staining positively for antibodies to IL-17 and (1C5–1C8) cells staining positively for IFNγ. Original magnification was × 400. Bar Graphs show cell counts and statistical comparisons based on one-way ANOVA. Hematoxylin and eosin (H&E) stained sections show infiltration of mononuclear cells in white matter of EAE (1C10) and EAE + GA (1C11) mice. However, the number of inflammatory pockets and inflammatory cells is fewer in EAE + GA compared to EAE. Normal (1C9) mice show no inflammatory infiltrates. (1C12) The number of positive quadrants with inflammation was scored and expressed as a percentage of the total number of quadrants (H&E; n = 4).

increased in EAE $P > 0.05$ but reduced by GA treatment, $P < 0.05$ (Fig. 1C4). The number of cells expressing IFN-g was increased in EAE $P < 0.001$ but reduced by GA treatment $P < 0.001$ (Fig. 1C8).

Inflammatory cell infiltration was examined in H&E-stained sections of spinal cord from mice euthanized on day 30 (1C9–1C11). While normal mice did not have cellular infiltration, EAE mice had 47.09 ± 1.86% of white matter with inflammation compared to 12.95 ± 2.34% in EAE + GA (Fig. 1C12, $P < 0.0001$).

Demyelination was assessed in sections of spinal cord using Luxol Fast Blue (LFB) staining (Fig. 1B5–B7). Quantitative analysis of the extent of demyelination shows 40.99 ± 2.7% of white matter with myelin loss (demyelination) in EAE as compared to 8.62 ± 2.4% in EAE + GA ($P < 0.0001$) (Fig. 1B4). These results were confirmed using immunohistochemical analysis with antibodies against myelin basic protein (MBP) (Fig. 1B5–B7). Quantitative analysis of the percentage of white matter with MBP loss showed significant loss in EAE that was reduced by GA treatment (Fig. 1B8). The changes in demyelination were confirmed qualitatively by transmission electron microscopy at 6500x (Fig. 1B9–B11).

Endoplasmic Reticulum (ER) Stress is increased in EAE spinal cord (Fig. 2). We examined ER stress by assessing cells expressing CCAAT-enhancer-binding protein homologous protein (CHOP), which is induced by ER stress and is a mediator of apoptosis[34]. The number of cells positive for CHOP was increased in EAE but decreased in EAE mice treated with GA (Fig. 2A1–A3). Figure 2A4 shows the quantitative analysis

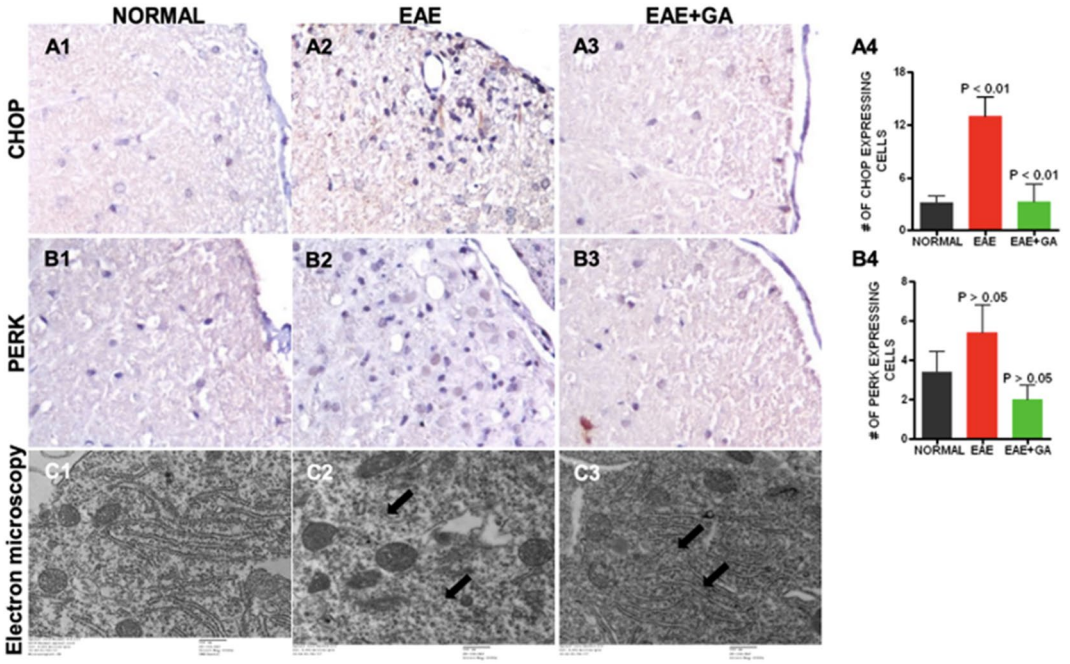

Figure 2. Endoplasmic reticulum stress seen in EAE was reduced by GA treatment. Endoplasmic reticulum stress was assessed with antibodies to CHOP (A1–A4) and PERK (B1–B4). Panels 1–3 show representative staining patterns in each treatment group for each antibody. Original magnification: X400. Panel 4 in each case shows a graph of the mean number of positive cells per field for each treatment group (CHOP: n = 4; PERK: n = 4) with intergroup comparisons based on a one-way ANOVA. Transmission electron microscopic examination (C1–C3) showed vesiculated endoplasmic reticulum, irregularly arranged and disrupted endoplasmic reticulum (arrows) in untreated EAE (C2) while regular and parallel organized endoplasmic reticulum in normal (C1) and GA treated EAE mice (C3).

of CHOP expression, which was significantly decreased in EAE + GA compared to EAE ($P < 0.01$). Next we examined ER stress in sections of the spinal cord using antibodies to protein kinase RNA-like endoplasmic reticulum (PERK) a component of mitochondria-associated ER membranes[35]. The number of cells positive for the PERK was increased in EAE but decreased in EAE mice treated with GA (Fig. 2B1–B3). Figure 2B4 shows the quantitative analysis of GFAP expression, which was significantly decreased in EAE + GA compared to EAE. Finally, we examined the structural integrity of the endoplasmic reticulum using transmission electron microscopy with 6500 × magnification and found ER disruption in EAE that was not present in normal or GA treated EAE (Fig. 22C1–C3).

Glatiramer acetate treatment improves mitochondrial function, fission/fusion, and biogenesis in EAE spinal cord (Fig. 3). *Mitochondrial integrity* was assessed by immunohistochemical and immunofluorescent staining. Function was assessed using expressions of PINK-1 and PARKIN. PINK-1 accumulates on poorly functioning (depolarized) mitochondria allowing PARKIN to bind, targeting the mitochondria for autophagy[36]. PINK-1 and PARKIN were increased in untreated EAE but not in EAE treated with GA (Fig. 3A1–A3 and B1–B3), confirming lost mitochondrial integrity in EAE and revealing that GA can restore this. Figure 3A4 and B4 shows the quantitative analysis of PGC1-α expression.

Mitochondrial biogenesis was examined in spinal cords for cells expressing PGC1-α, a mediator of mitochondrial biogenesis[37], by immunohistochemistry (Fig. 3C1–C3). Figure 3C4 shows the quantitative analysis of PGC1-α expression, which was significantly reduced in EAE mice $P < 0.01$, but restored back to normal levels in EAE mice treated with GA ($P < 0.01$).

Morphological changes in mitochondria were assessed directly by transmission electron microscopy at 6500X magnification (Figure D1–D3). Mitochondrial fission, cristae damage and loss, mitochondrial membrane damage and disappearance, and changes in size and shape were seen in EAE mice but not in the tissues from normal mice or EAE mice treated with GA. Mitochondrial fusion was not seen.

Mitochondrial fusion, which is reduced under conditions of ER stress, was assessed by immunohistofluorescence staining (Fig. 3E1–E3) and western blot analysis for MFN-2, a marker of fusion[38]. The number of cells positive for the MFN-2 was reduced in EAE ($P < 0.05$) but not in EAE mice treated with GA compared to normal mice ($P < 0.05$) (Fig. 3E4).

Mitochondrial fission, which is increased under conditions of mitochondrial stress, was assessed by immunofluorescence staining for FIS-1[39] and both immunohistochemistry and western blot analysis for DNM1-L (Fig. 3F1–F3 and G1-3G3, 3G5)[40]. The number of cells expressing FIS-1 did not change in the EAE mice but significantly decreased in EAE mice treated with GA compared to control EAE mice ($P < 0.05$) (Fig. 3F4). The

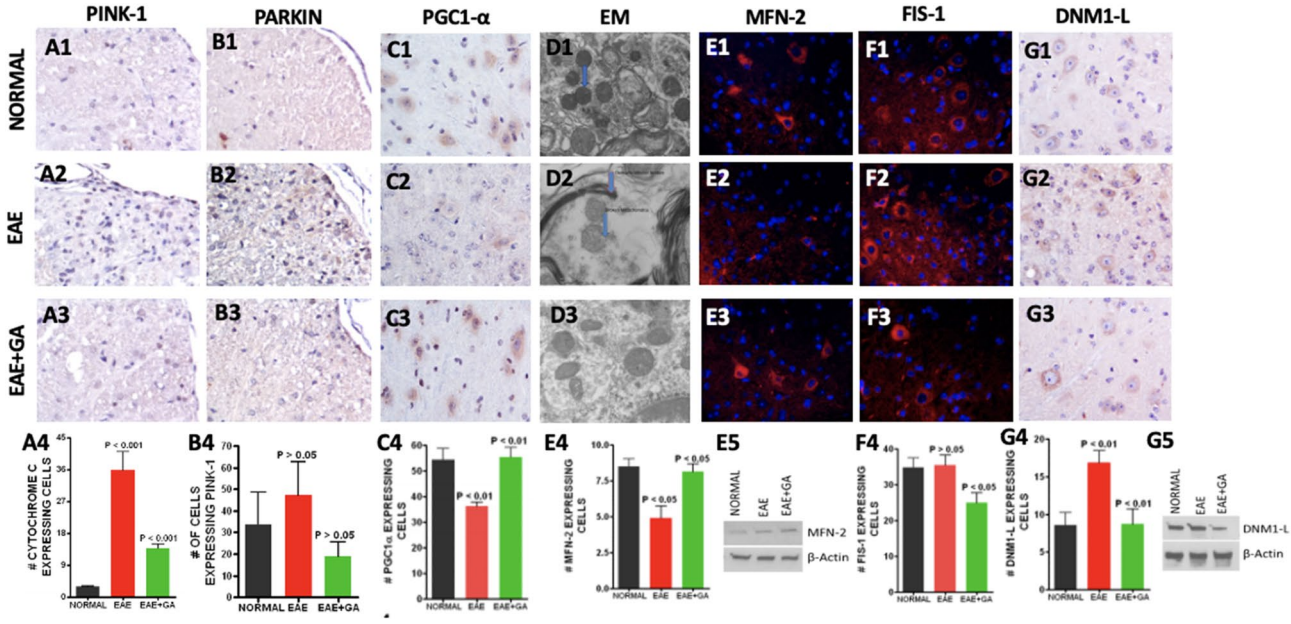

Figure 3. Glatiramer Acetate treatment improves mitochondrial function, fission/fusion, and biogenesis in EAE mice. (A,B) EAE caused loss of mitochondrial integrity that was reduced by GA treatment. Mitochondrial integrity was assessed by staining for PINK-1 (A1–A4) and staining for PARKIN (B1–B4). Panels 1–3 show representative staining patterns in each treatment group for each antibody. Original magnification: X400. Panel 4 in each case shows a graph of the mean number of positive cells per field for each treatment group (n = 4) with intergroup comparisons based on a one-way ANOVA. (C, D) Changes in mitochondrial biogenesis and morphology in EAE are reduced by GA treatment. Mitochondrial biogenesis was assessed with antibody to PGC1-α, a regulator of mitochondrial biogenesis (C1–C4) Panels 1–3 show representative staining patterns in each treatment group for each antibody. Original magnification: X400. Panel 4 shows a graph of the mean number of positive cells per field for each treatment group (n = 3; n = 4) with intergroup comparisons based on a one-way ANOVA. Mitochondrial morphology was assessed by transmission electron microscopy (TEM) at 6500 × magnification. Morphological changes were observed in mitochondria in EAE (D2) that were reduced by treatment (D3) compared to the mitochondria in normal mice (D1). In EAE many of the mitochondria showed mitochondrial membrane disruption with disruption or loss of cristae and changes in mitochondrial size and shape with increased fission. The results shown are typical of at least 3 grids for each mouse (n = 5). (E–G) EAE caused changes in mitochondrial dynamics that were reduced by GA treatment. Mitochondrial fusion was assessed by staining with antibody to Mitofusin–2 (MFN-2) (E1–E4) and mitochondrial fission was assessed with antibody to FIS-1 (F1–F4) and DNM1-L (G1–G4). Panels 1 to 3 show representative staining patters in each treatment group with each antibody. Original magnification was × 400. Panel 4 in each case shows a graph of the mean number of positive cells per field for each treatment group (MFN-2, n = 4; FIS-1, n = 3; DNM1-L, n = 3) with intergroup comparisons based on a one-way ANOVA. (E5) Western Blot anasupplemental filelysis of mitochondrial fraction of spinal cord shows an increase in MFN-2 in the EAE + GA mice compared to EAE and Normal. (G5) Western Blot analysis of mitochondrial fraction of spinal cord shows a decrease in DNM1-L in the EAE + GA mice compared to EAE and Normal. Full length membranes of the blots for MNF-2 and DNM1-L are provided as a . Full length membranes of the blots for B-actin are unable to be provided as the team only saved the files of the cropped images.

number of cells expressing DNM1-L significantly increased in the EAE mice ($P < 0.01$) but decreased to normal levels in EAE + GA ($P < 0.01$) (Fig. 3G4).

Changes in the mitochondria associated membrane (MAM) associated with EAE were reduced by GA treatment (Fig. 4). Mitochondria and the endoplasmic reticulum interact through a specialized domain on the ER called the mitochondria-associated membranes (MAM). Several proteins are located in MAMs, including PACS-2, VDAC-1[41,42]. We examined PACS-2 and VDAC-1 expressions in EAE using immunohistochemistry and evaluated the effect of GA treatment (Fig. 4A1–A3 and 4B1–4B3). Numbers of cells expressing PACS-2 and VDAC-1 (Fig. 4A4 and B4) were increased in EAE ($P < 0.05$) but returned toward normal in GA treated mice ($P < 0.05$).

Glatiramer Acetate treatment increases activity of the NAD+ dependent pathway in EAE spinal cord (Fig. 5). Because of the importance of NAD regulation in mitochondrial function and cell survival[43] we examined expression of Nicotinamide phosphoribosyltransferase (NAMPT), the rate limiting enzyme in NAD biosynthesis[44], and Sirtuins 1 and 3 which are NAD dependent protein deacetylases[45] which play a role in mitochondrial dynamics. Staining for NAMPT, SIRT-1 and SIRT-3 and was reduced in EAE compared to normal

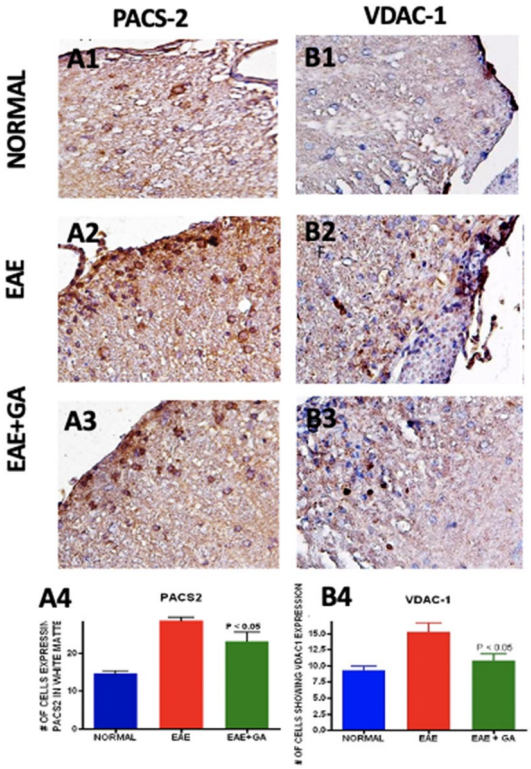

Figure 4. Changes in the mitochondria associated membrane (MAM) associated with EAE were reduced by GA treatment. Antibodies to PACS2 (A1–A4) and VDAC-1 (B1–B4) were studied as markers of the MAM. (A1–A3 and B1–B3) show the antibody staining in each treatment group with each antibody at an original magnification of × 400. (A4 and B4) show quantitation of staining in each treatment group with comparisons by one-way ANOVA (n = 5).

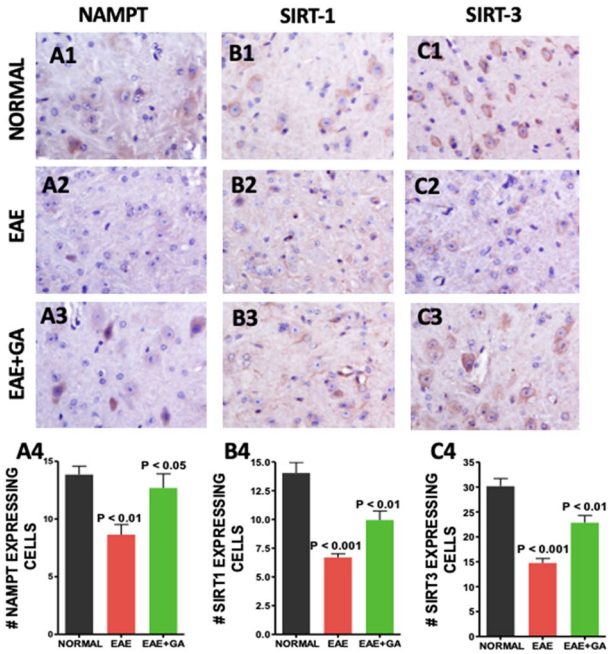

Figure 5. EAE associated reductions in NAD-dependent pathways were reduced by GA treatment. NAD+ dependent pathways were assessed with antibodies to NAMPT (A1–A4), Sirt-1 (B1–B4), and Sirt-3 (C1–C4). For each antibody, panels 1–3 show typical staining in each treatment group at an original magnification of × 400 and panel 4 is a graph of the quantification of positive cells in the spinal cord with comparisons made using one-way ANOVA (n = 4).

(Fig. 5A2, B2, C2). Treatment with GA partially restored levels of NAMPT, SIRT-1 and SIRT-3 (Fig. 5A3, B3, C3). Figure 5A4, B4 and C4 show the quantitative analysis of NAMPT, SIRT-1 and SIRT-3 expressions.

Apoptosis is increased in EAE mouse spinal cord (Fig. 6). Because of mitochondrial involvement in programmed cell death, we assessed apoptosis in EAE using the TUNEL assay. TUNEL cells were significantly increased in EAE ($P<0.001$) but lower in EAE + GA spinal cords ($P<0.001$) (Fig. 6A1–A3). Figure 6A4 shows the quantitative analysis of TUNEL positive cells in the gray matter of these spinal cords. To evaluate activation of the apoptosis pathway we examined the expression of FOXO-1, a transcription factor regulated by AKT and implicated in apoptosis[46] in part by the regulation of Bax, an activator of apoptosis[47]. FOXO-1 expressing cells were increased in EAE ($P<0.05$) but normal in GA treated mice ($P<0.001$) (Fig. 6B1–B4). BCL-2 expressing cells were increased in EAE ($P<0.05$) but lower after GA treatment ($P<0.05$) (Fig. 6C1–C4). Staining for cytochrome-C expression in spinal cord sections was used as a measure of apoptosis triggered by decreased mitochondrial integrity[48] (Fig. 6D1–D3). Cytochrome C expressing cells were increased in EAE ($P<0.001$) but was reduced back to normal levels in GA treated mice ($P<0.001$) (Fig. 6D4).

Discussion

In this study, we investigated the effects of GA, a polypeptide-based approved drug for the treatment of MS, on ER stress and mitochondrial dysfunction in the spinal cord of EAE mice. Our principal findings are: (1) as expected, GA improved clinical score, reduced inflammatory activity, and promoted remyelination; (2) GA reduced ER stress; (3) GA improves mitochondrial function, reduces mitochondrial fission, increases mitochondrial fission, and increases mitochondrial biogenesis; (4) GA regulated changes in mitochondrial associated membranes; (5) GA increases activity of the NAD+ dependent pathway; and (6) GA reduces apoptosis. Our findings strongly suggest that GA can indirectly mediate ER-stress and the downstream effects of the unfolded protein response in the EAE model.

Research thus far has demonstrated that GA exerts its immunomodulatory effects by altering T-cell differentiation through promotion of Th2-polarized GA-reactive CD4+ T-cells[49]. Furthermore, induction of Th2 cells in the periphery during GA treatment leads to reduced inflammation, and in turn promotes remyelination and neuronal survival[50]. Figure 1 of our research confirms these findings. Specifically, we showed that GA

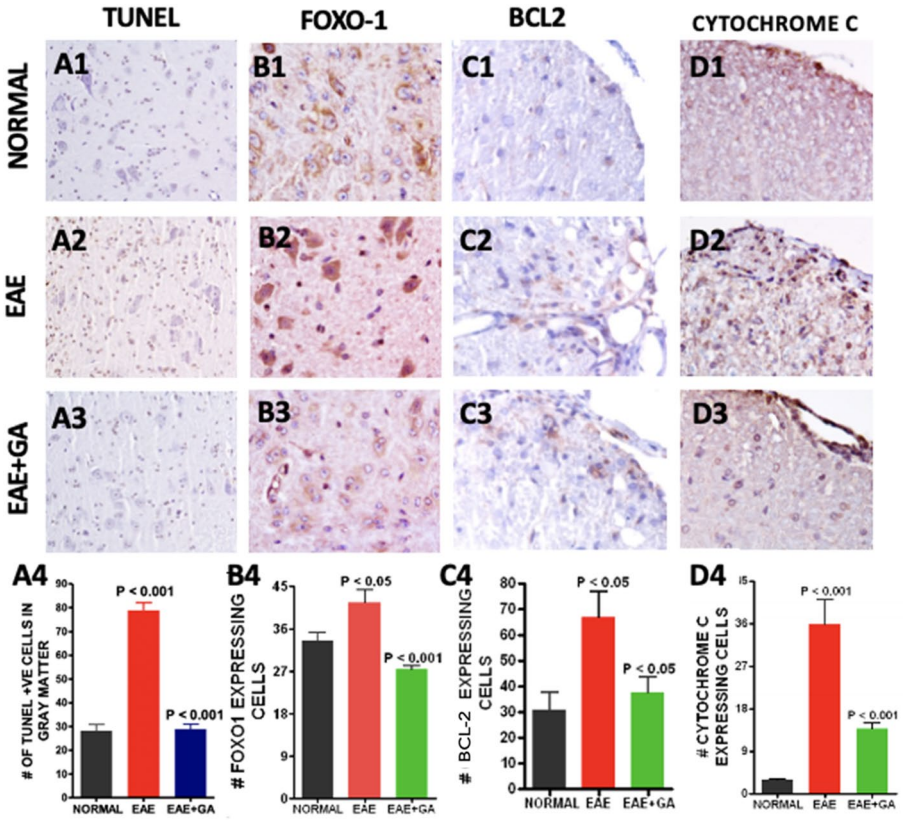

Figure 6. EAE related increases in apoptosis were reduced by GA treatment. Apoptosis was assessed in spinal cord tissue with in situ TUNEL staining (A1–A4) and with antibodies to FOXO-1 (B1–B4), BAX (C1–C4), and Cytochrome C (D1–D4). Panels 1–3 show typical staining patterns for each treatment group at an original magnification of × 400 while panels 4 provide quantitation of numbers of positive cells in each group (n = 4) with comparisons using one-way ANOVA.

downregulated expression of IFN-y, which promotes myelin damage by stimulating inflammation. It is important to note that GA is degraded in the periphery and cannot cross the blood brain barrier, so the spinal cord findings that we present demonstrate the in situ bystander effect of GA[27].

ER stress is characterized by the accumulation of misfolded proteins, resulting in chronic perturbations to ER homeostasis. The unfolded protein response (UPR) is an evolutionary conserved process that is activated in order to restore ER homeostasis by correcting protein-folding machinery. The UPR has three main arms led by ER-transmembrane proteins: PERK, IRE1, and ATF6. In this study, we focused specifically on PERK and its downstream apoptotic gene CHOP. Although ER stress initially acts as self-preservation, chronic ER stress and activation of the UPR leads to cellular apoptosis[21]. It is widely known that the UPR is activated in both MS and EAE lesions, induced by elevated levels of proinflammatory mediators, and contributes to disease progression[51]. Specifically, previous studies have demonstrated that EAE, including spinal cord tissue, exhibits upregulated levels of p-PERK and CHOP in oligodendrocytes, T cells, astrocytes, and macrophages/ microglia[41,51–53]. We confirmed this using immunostaining and showed that these changes were reversed with GA treatment. This reversal effect was further supported by electron microscopy which demonstrated restored ER structure similar to that of wild type mice. We suggest that this is due to GA's ability to mediate neuroinflammation, specifically IFN-y. IFN-y has previously been shown to induce PERK activation and its downstream translation initiation factor 2 (eIF2α), and IFN-y induced apoptosis in rat oligodendrocytes is associated with ER stress[54]. PERK and CHOP are implicated in the regulation of Th17 inflammatory cytokines, and one study specifically found that inhibiting PERK inhibits Th17 cell differentiation[55,56] Targeting the PERK-eIF2α pathway has been reported as an ideal strategy for protecting oligodendrocyte protection in MS, and we show for the first time that GA may be able to[57]. Other chemical compounds that have been shown to activate this pathway and are neuroprotective in EAE and MS include salburnal[58] and guanabenz[59]. Future studies with GA should investigate its cytoprotective effects on other branches of the UPR in specifically oligodendrocytes and neurons.

Mitochondrial dysfunction is a pathological hallmark in EAE and MS lesions, and it is well associated with ER stress[16,17]. Therefore, we were interested in examining changes in mitochondrial dynamics to determine if GA would reverse such changes, possibly through attenuation of the ER-stress induced UPR. The PERK-ATF4-CHOP pathway exerts regulatory effects on the expression of Parkin, a critical regulator in mitochondrial dynamics (Sarrabeth Stone 2015). Parkin plays a role in mitochondrial dynamics[60,61], bioenergetics[62,63], and mitophagy[36]. Parkin also is known to modulate MAMs, which we assessed by staining for PACS2 and VDAC1, to maintain calcium transfer between the ER and mitochondria[62]. Haile et al. recently showed that during MS progression, ER stress is strongly associated with the upregulation of Rab32, a GTPase that regulates MAMs, and contributes to neuronal death. We found that both the PINK1/Parkin pathway and MAMs was upregulated in the EAE model as found previously[64], and GA reversed this, likely by suppressing the PERK branch of the UPR.

The UPR, PINK1/Parkin pathway, and MAMs all play a role in mitochondrial fission/fusion processes. ER-stress induced PERK regulates the Drp1–Fis1 complex through control of the adaptor protein AKAP121. PINK1 and Parkin promote mitochondrial fission via a Drp1-mediated mechanism[65]. Parkin also negatively regulates mitochondrial fusion via MFN2 by ubiquitination[66] and interestingly, MFN2 deficiency is actually associated with contributing to the UPR response as well as cellular apoptosis because MFN2 plays a role in repressing PERK[67,68]. Previous studies have also demonstrated that ER-mitochondrial tethering can contribute to the upregulation of Drp-mediated fission via formation of constriction sites[69,70]. Recently, it was found that Drp1 is activated in experimental models for multiple sclerosis, and inhibition of its pathological hyperactivation is neuroprotective[71]. For the first time, we show that GA reduces mitochondrial fission activity and increases fusion activity in EAE mice, again strongly suggesting that GA targets ER stress and downstream mitochondrial mediators.

To further explore the effects of EAE and treatment of EAE with immunomodulating therapy on metabolism we examined expression of nicotinamide phosphoribosyltransferase (NAMPT), the rate limiting step in the NAD+ salvage pathway which has neuroprotective effects[44] and Sirt 1 and 3, members of the Sirtuin family which are NAD dependent protein deacetylases which are key metabolic sensors in the stress response[45]. Increasing SIRT1 activity, either by treatment with the Sirt activator, resveratrol[72] or by genetic overexpression[28], reduces the clinical and pathological severity of EAE. SIRT3 activates PGC-1α which stimulates mitochondrial biogenesis and is associated with ROS suppression and neuroprotection[73]. Sirt1 is of further interest because levels are reduced in peripheral blood mononuclear cells during relapses of MS[74] and were restored by treatment with GA[75]. Sirt3 changes are also implicated in MS in that levels were reduced in non-lesioned grey matter from MS brains[76]. We found that expression of NAMPT and Sirt 1 and 3 were reduced in EAE and restored or partially restored to normal levels by treatment with immunomodulating therapy with glatiramer acetate. This suggests that such therapy can restore cells to a more normal metabolic state.

To determine whether the reductions in ER stress, mitochondrial dysfunction and metabolic abnormalities induced by immunomodulatory therapy were associated with reductions in cellular death we examined apoptosis and changes in related pathways. The increased fission processes that we found in the EAE model can contribute to cellular apoptosis by the opening of BAX lined pores and release of cytochrome C[77], and our findings supported this. Using TUNEL staining we found that immunomodulating therapy with GA reduced the high levels of apoptosis is found in untreated EAE. We studied the expression of forkhead box O (FOXO), transcription factors implicated in the regulation of apoptosis[46] and found it to be upregulated in EAE and the opposite effect in GA treated groups. We examined the expression of Bax, a BCL-2 family member that promotes apoptosis by contributing to mitochondrial membrane pore formation[47] and found increased levels in EAE which were reversed by GA treatment. These results show that while EAE is associated with an increase in cell death, treatment with the immunomodulating therapy, GA, is associated with a reduction. Our results strengthen the idea that the mitochondrial and ER changes in EAE are part of a coordinated response to metabolic stress caused by inflammation and that immunomodulating therapy can reduce that stress.

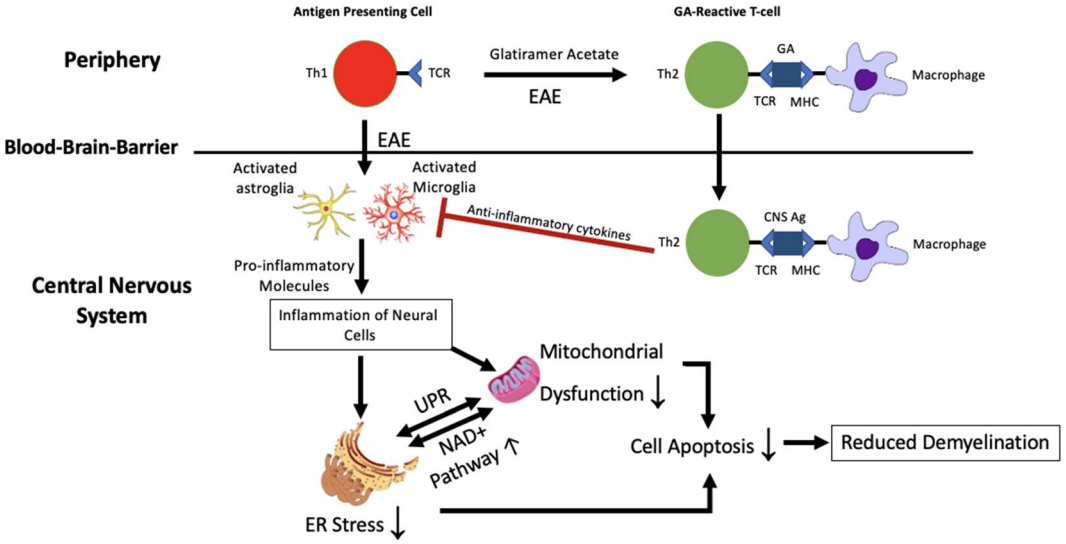

Figure 7. Proposed neuroprotective mechanism underlying glatiramer acetate treatment in EAE. GA induces a shift towards the Th2 response in the CNS. This reduced inflammatory environment contributes to controlling the synergistic ER stress response and mitochondrial dysfunction. By doing so, apoptotic activity in the CNS is downregulated, and in turn, disease progression is slowed. CNS AG: CNS antigen; MHC: major histocompatibility complex; TCR: T cell receptor.

Conclusion

We found mitochondrial dysfunction, endoplasmic reticulum stress and disrupted NAD metabolism in the spinal cords of EAE mice. For the first time, we show that GA can potentially reverse these pathological changes. Given that the direct effects of GA are thought to be in the peripheral immune system, it seems likely that the observed changes are an indirect effect of the immunomodulatory effect resulting in reduced inflammation in the spinal cord. The reduction in neuronal apoptosis in EAE upon GA treatment could be a result of ameliorated ER stress, improved mitochondrial function, and regulated NAD metabolism. Figure 7 shows our proposed mechanism.

Data availability

The primary data upon which this manuscript is based is available from the corresponding author upon reasonable request.

Received: 21 July 2022; Accepted: 11 February 2023
Published online: 06 April 2023

References

1. Lassmann, H., Brück, W. & Lucchinetti, C. F. The immunopathology of multiple sclerosis: An overview. *Brain Pathol.* **17**, 210–218 (2007).
2. Rottlaender, A. & Kuerten, S. Stepchild or prodigy? Neuroprotection in multiple sclerosis (MS) research. *Int. J. Mol. Sci.* **16**, 14850–14865 (2015).
3. Jäger, A., Dardalhon, V., Sobel, R. A., Bettelli, E. & Kuchroo, V. K. Th1, Th17, and Th9 effector cells induce experimental autoimmune encephalomyelitis with different pathological phenotypes. *J. Immunol.* **183**, 7169–7177 (2009).
4. Hendriks, J. J. A., Teunissen, C. E., de Vries, H. E. & Dijkstra, C. D. Macrophages and neurodegeneration. *Brain Res.Rev.* **48**, 185–195. https://doi.org/10.1016/j.brainresrev.2004.12.008 (2005).
5. Matthews, P. M. *et al.* Putting magnetic resonance spectroscopy studies in context: Axonal damage and disability in multiple sclerosis. *Semin. Neurol.* **18**, 327–336 (1998).
6. Trapp, B. D. *et al.* Axonal transection in the lesions of multiple sclerosis. *N. Engl. J. Med.* **338**, 278–285 (1998).
7. Wujek, J. R. *et al.* Axon loss in the spinal cord determines permanent neurological disability in an animal model of multiple sclerosis. *J. Neuropathol. Exp. Neurol.* **61**, 23–32. https://doi.org/10.1093/jnen/61.1.23 (2002).
8. Lassmann, H., van Horssen, J. & Mahad, D. Progressive multiple sclerosis: Pathology and pathogenesis. *Nat. Rev. Neurol.* **8**, 647–656 (2012).
9. Soulika, A. M. *et al.* Initiation and progression of axonopathy in experimental autoimmune encephalomyelitis. *J. Neurosci.* **29**, 14965–14979 (2009).
10. Goodin, D. S. Disease-modifying therapy in multiple sclerosis: Update and clinical implications. *Neurology* **71**, S8-13 (2008).
11. Dutta, R. & Trapp, B. D. Mechanisms of neuronal dysfunction and degeneration in multiple sclerosis. *Prog. Neurobiol.* **93**, 1–12 (2011).
12. Jacobsen, C. *et al.* Brain atrophy and disability progression in multiple sclerosis patients: A 10-year follow-up study. *J. Neurol. Neurosurg. Psychiatry* **85**, 1109–1115 (2014).
13. Witte, M. E., Mahad, D. J., Lassmann, H. & van Horssen, J. Mitochondrial dysfunction contributes to neurodegeneration in multiple sclerosis. *Trends Mol. Med.* **20**, 179–187 (2014).
14. van Horssen, J., Witte, M. E. & Ciccarelli, O. The role of mitochondria in axonal degeneration and tissue repair in MS. *Mult. Scler.* **18**, 1058–1067 (2012).
15. Ciccarelli, O. *et al.* Spinal cord repair in MS: Does mitochondrial metabolism play a role?. *Neurology* **74**, 721–727 (2010).

16. Cunnea, P. *et al.* Expression profiles of endoplasmic reticulum stress-related molecules in demyelinating lesions and multiple sclerosis. *Mult. Scler.* **17**, 808–818 (2011).
17. Roussel, B. D. *et al.* Endoplasmic reticulum dysfunction in neurological disease. *Lancet Neurol.* **12**, 105–118 (2013).
18. Bravo, R. *et al.* Increased ER-mitochondrial coupling promotes mitochondrial respiration and bioenergetics during early phases of ER stress. *J. Cell Sci.* **124**, 2143–2152 (2011).
19. Csordás, G. *et al.* Structural and functional features and significance of the physical linkage between ER and mitochondria. *J. Cell Biol.* **174**, 915–921. https://doi.org/10.1083/jcb.200604016 (2006).
20. Csordás, G. *et al.* Imaging interorganelle contacts and local calcium dynamics at the ER-mitochondrial interface. *Biophys. J.* **98**, 381a. https://doi.org/10.1016/j.bpj.2009.12.2053 (2010).
21. Andhavarapu, S., Mubariz, F., Arvas, M., Bever, C. Jr. & Makar, T. K. Interplay between ER stress and autophagy: A possible mechanism in multiple sclerosis pathology. *Exp. Mol. Pathol.* **108**, 183–190 (2019).
22. Sanchez, C. L., Sims, S. G., Nowery, J. D. & Meares, G. P. Endoplasmic reticulum stress differentially modulates the IL-6 family of cytokines in murine astrocytes and macrophages. *Sci. Rep.* **9**, 1–12 (2019).
23. Arnon, R. & Sela, M. Immunomodulation by the copolymer glatiramer acetate. *J. Mol. Recog.* **16**, 412–421. https://doi.org/10.1002/jmr.628 (2003).
24. Aharoni, R., Teitelbaum, D., Sela, M. & Arnon, R. Copolymer 1 induces T cells of the T helper type 2 that crossreact with myelin basic protein and suppress experimental autoimmune encephalomyelitis. *Proc. Natl. Acad. Sci.* **94**, 10821–10826. https://doi.org/10.1073/pnas.94.20.10821 (1997).
25. Duda, P. W., Schmied, M. C., Cook, S. L., Krieger, J. I. & Hafler, D. A. Glatiramer acetate (Copaxone) induces degenerate, Th2-polarized immune responses in patients with multiple sclerosis. *J. Clin. Investig.* **105**, 967–976 (2000).
26. Aharoni, R., Kayhan, B., Eilam, R., Sela, M. & Arnon, R. Glatiramer acetate-specific T cells in the brain express T helper 2/3 cytokines and brain-derived neurotrophic factor in situ. *Proc. Natl. Acad. Sci.* **100**, 14157–14162. https://doi.org/10.1073/pnas.2336171100 (2003).
27. Aharoni, R. *et al.* Demyelination arrest and remyelination induced by glatiramer acetate treatment of experimental autoimmune encephalomyelitis. *Proc. Natl. Acad. Sci. USA* **105**, 11358–11363 (2008).
28. Nimmagadda, V. K. *et al.* Overexpression of SIRT1 protein in neurons protects against experimental autoimmune encephalomyelitis through activation of multiple SIRT1 targets. *J. Immunol.* **190**, 4595–4607 (2013).
29. Gerzanich, V. *et al.* Salutary effects of glibenclamide during the chronic phase of murine experimental autoimmune encephalomyelitis. *J. Neuroinflammation* **14**, 1–18 (2017).
30. Bryant, J. L. *et al.* Renal aquaporin-4 associated pathology in TG-26 mice. *Exp. Mol. Pathol.* **104**, 239–249 (2018).
31. Bryant, J. *et al.* 7,8-Dihydroxyflavone improves neuropathological changes in the brain of Tg26 mice, a model for HIV-associated neurocognitive disorder. *Sci. Rep.* **11**, 18519 (2021).
32. Makar, T. *et al.* A subset of mobilized human hematopoietic stem cells express germ layer lineage genes which can be modulated by culture conditions. *Stem Cell Res. Ther.* **9**, 1–10 (2018).
33. ImageJ. https://imagej.nih.gov/ij/.
34. Nishitoh, H. CHOP is a multifunctional transcription factor in the ER stress response. *J. Biochem.* **151**, 217–219 (2012).
35. Liu, Z., Lv, Y., Zhao, N., Guan, G. & Wang, J. Protein kinase R-like ER kinase and its role in endoplasmic reticulum stress-decided cell fate. *Cell Death Dis.* **6**, e1822 (2015).
36. Narendra, D. P. *et al.* PINK1 is selectively stabilized on impaired mitochondria to activate Parkin. *PLoS Biol.* **8**, e1000298 (2010).
37. Kong, X. *et al.* Sirtuin 3, a New Target of PGC-1α, plays an important role in the suppression of ROS and mitochondrial biogenesis. *PLoS ONE* **5**, e11707. https://doi.org/10.1371/journal.pone.0011707 (2010).
38. Chen, H. *et al.* Mitofusins Mfn1 and Mfn2 coordinately regulate mitochondrial fusion and are essential for embryonic development. *J. Cell Biol.* **160**, 189–200 (2003).
39. Mai, S., Klinkenberg, M., Auburger, G., Bereiter-Hahn, J. & Jendrach, M. Decreased expression of Drp1 and Fis1 mediates mitochondrial elongation in senescent cells and enhances resistance to oxidative stress through PINK1. *J. Cell Sci.* **123**, 917–926 (2010).
40. Cerveny, K. L., McCaffery, J. M. & Jensen, R. E. Division of mitochondria requires a novel DNM1-interacting protein, Net2p. *Mol. Biol. Cell* **12**, 309–321 (2001).
41. Deslauriers, A. M. *et al.* Neuroinflammation and endoplasmic reticulum stress are coregulated by crocin to prevent demyelination and neurodegeneration. *J. Immunol.* **187**, 4788–4799. https://doi.org/10.4049/jimmunol.1004111 (2011).
42. Haile, Y. *et al.* Rab32 connects ER stress to mitochondrial defects in multiple sclerosis. *J. Neuroinflammation* **14**, 19 (2017).
43. Yang, H. *et al.* Nutrient-sensitive mitochondrial NAD+ levels dictate cell survival. *Cell* **130**, 1095–1107 (2007).
44. Garten, A. *et al.* Physiological and pathophysiological roles of NAMPT and NAD metabolism. *Nat. Rev. Endocrinol.* **11**, 535–546. https://doi.org/10.1038/nrendo.2015.117 (2015).
45. Li, X. & Kazgan, N. Mammalian sirtuins and energy metabolism. *Int. J. Biol. Sci.* **7**, 575–587 (2011).
46. Zhang, X., Tang, N., Hadden, T. J. & Rishi, A. K. Akt, FoxO and regulation of apoptosis. *Biochim. Biophys. Acta* **1813**, 1978–1986 (2011).
47. Westphal, D., Kluck, R. M. & Dewson, G. Building blocks of the apoptotic pore: How Bax and Bak are activated and oligomerize during apoptosis. *Cell Death Differ.* **21**, 196–205 (2014).
48. Garrido, C. *et al.* Mechanisms of cytochrome c release from mitochondria. *Cell Death Differ.* **13**, 1423–1433 (2006).
49. Weber, M. S., Hohlfeld, R. & Zamvil, S. S. Mechanism of action of glatiramer acetate in treatment of multiple sclerosis. *Neurotherapeutics* **4**, 647 (2007).
50. Filippi, M. *et al.* Glatiramer acetate reduces the proportion of new MS lesions evolving into 'black holes'. *Neurology* **57**, 731–733 (2001).
51. Lin, W. & Popko, B. Endoplasmic reticulum stress in disorders of myelinating cells. *Nat. Neurosci.* **12**, 379–385 (2009).
52. Meares, G. P. *et al.* PERK-dependent activation of JAK1 and STAT3 contributes to endoplasmic reticulum stress-induced inflammation. *Mol. Cell. Biol.* **34**, 3911–3925 (2014).
53. Ní Fhlathartaigh, M. *et al.* Calreticulin and other components of endoplasmic reticulum stress in rat and human inflammatory demyelination. *Acta Neuropathol. Commun.* **1**, 37 (2013).
54. Lin, W., Harding, H. P., Ron, D. & Popko, B. Endoplasmic reticulum stress modulates the response of myelinating oligodendrocytes to the immune cytokine interferon-γ. *J. Cell Biol.* **169**, 603 (2005).
55. Brucklacher-Waldert, V. *et al.* Cellular stress in the context of an inflammatory environment supports TGF-β-independent T helper-17 differentiation. *Cell Rep.* **19**, 2357 (2017).
56. Kemp, K. & Poe, C. Stressed: The unfolded protein response in T cell development, activation, and function. *Int. J. Mol. Sci.* **20**, 1792 (2019).
57. Sarrabeth Stone, W. L. The unfolded protein response in multiple sclerosis. *Front. Neurosci.* **9**, 264 (2015).
58. Lin, W. *et al.* Enhanced integrated stress response promotes myelinating oligodendrocyte survival in response to interferon-gamma. *Am. J. Pathol.* **173**, 1508–1517 (2008).
59. Way, S. W. *et al.* Pharmaceutical integrated stress response enhancement protects oligodendrocytes and provides a potential multiple sclerosis therapeutic. *Nat. Commun.* **6**, 6532 (2015).
60. Deng, H., Dodson, M. W., Huang, H. & Guo, M. The Parkinson's disease genes pink1 and parkin promote mitochondrial fission and/or inhibit fusion in Drosophila. *Proc. Natl. Acad. Sci.* **105**, 14503–14508. https://doi.org/10.1073/pnas.0803998105 (2008).

61. Poole, A. C. *et al.* The PINK1/Parkin pathway regulates mitochondrial morphology. *Proc. Natl. Acad. Sci. USA* **105**, 1638–1643 (2008).
62. Calì, T., Ottolini, D., Negro, A. & Brini, M. Enhanced parkin levels favor ER-mitochondria crosstalk and guarantee Ca(2+) transfer to sustain cell bioenergetics. *Biochim. Biophys. Acta* **1832**, 495–508 (2013).
63. Witte, M. E. *et al.* Parkinson's disease-associated parkin colocalizes with Alzheimer's disease and multiple sclerosis brain lesions. *Neurobiol. Dis.* **36**, 445–452 (2009).
64. Lieberknecht, V. *et al.* Pramipexole, a dopamine D2/D3 receptor-preferring agonist, prevents experimental autoimmune encephalomyelitis development in mice. *Mol. Neurobiol.* **54**, 1033–1045 (2016).
65. Buhlman, L. *et al.* Functional interplay between Parkin and Drp1 in mitochondrial fission and clearance. *Biochim. Biophys. Acta* **1843**, 2012–2026 (2014).
66. Ham, S. J. *et al.* Decision between mitophagy and apoptosis by Parkin via VDAC1 ubiquitination. *Proc. Natl. Acad. Sci. USA* **117**, 4281–4291 (2020).
67. Muñoz, J. P. *et al.* Mfn2 modulates the UPR and mitochondrial function via repression of PERK. *EMBO J.* **32**, 2348–2361 (2013).
68. McLelland, G.-L. *et al.* Mfn2 ubiquitination by PINK1/parkin gates the p97-dependent release of ER from mitochondria to drive mitophagy. *Elife* **7**, e32866 (2018).
69. van Vliet, A. R., Verfaillie, T. & Agostinis, P. New functions of mitochondria associated membranes in cellular signaling. *Biochimica et Biophysica Acta (BBA) Mol. Cell Res.* **1843**, 2253–2262. https://doi.org/10.1016/j.bbamcr.2014.03.009 (2014).
70. Kim, H. *et al.* Fine-tuning of Drp1/Fis1 availability by AKAP121/Siah2 regulates mitochondrial adaptation to hypoxia. *Mol. Cell* **44**, 532–544 (2011).
71. Luo, F., Herrup, K., Qi, X. & Yang, Y. Inhibition of Drp1 hyper-activation is protective in animal models of experimental multiple sclerosis. *Exp. Neurol.* **292**, 21 (2017).
72. Shindler, K. S. *et al.* Oral resveratrol reduces neuronal damage in a model of multiple sclerosis. *J. Neuro-Ophthalmol.* **30**, 328–339. https://doi.org/10.1097/wno.0b013e3181f7f833 (2010).
73. Giralt, A. *et al.* Peroxisome proliferator-activated receptor-γ coactivator-1α controls transcription of theSirt3Gene, an essential component of the thermogenic brown adipocyte phenotype. *J. Biol. Chem.* **286**, 16958–16966. https://doi.org/10.1074/jbc.m110.202390 (2011).
74. Tegla, C. A. *et al.* SIRT1 is decreased during relapses in patients with multiple sclerosis. *Exp. Mol. Pathol.* **96**, 139–148 (2014).
75. Hewes, D. *et al.* SIRT1 as a potential biomarker of response to treatment with glatiramer acetate in multiple sclerosis. *Exp. Mol. Pathol.* **102**, 191–197 (2017).
76. Rice, C. *et al.* SIRT3 expression is reduced in non-lesional grey matter in multiple sclerosis. (2013).
77. Yu, R., Lendahl, U., Nistér, M. & Zhao, J. Regulation of mammalian mitochondrial dynamics: Opportunities and challenges. *Front. Endocrinol.* **11**, 374 (2020).

Acknowledgements

This work was supported by grants from Teva Neuroscience, Inc. and the Department of Veteran's Affairs.

Author contributions

C.B. and T.M. designed the study. T.M. induced the E.A.E. in mice and injected the mice with glatiramer acetate. T.M. and V.N. euthanized the mice and collected the tissue. V.N., P.G., and S.A. performed the immunohistochemical staining. P.G. did the western blot analysis. S.R. prepared tissue for electron microscopy, took the pictures, and provided the analysis. T.M., S.A., V.N., K.K., V.G., M.S. and C.B. analyzed and interpreted the data. S.A and T.M. drafted the manuscript. All authors reviewed and approved the final version of the manuscript.

Competing interests

Partial funding for the study was provided by an investigator-initiated grant to Dr. Makar from Teva Neuroscience, Inc. which markets glatiramer acetate as a treatment for multiple sclerosis. Guda declares no competing interests. Ray declares no competing interests. Andhavarapu declares no competing interests. Keledjian declares no competing interests. Gerzanich declares no competing interests. Simard declares no competing interests. Nimmagadda declares no competing interests. Bever declares no competing interests.

Additional information

Supplementary Information The online version contains supplementary material available at https://doi.org/10.1038/s41598-023-29852-x.

Correspondence and requests for materials should be addressed to T.K.M.

Reprints and permissions information is available at www.nature.com/reprints.

Publisher's note Springer Nature remains neutral with regard to jurisdictional claims in published maps and institutional affiliations.